ISSN 1070-3284, Russian Journal of Coordination Chemistry, 2020, Vol. 46, No. 11, pp. 772–778. © Pleiades Publishing, Ltd., 2020.
Russian Text © The Author(s), 2020, published in Koordinatsionnaya Khimiya, 2020, Vol. 46, No. 11, pp. 698–705.

Dedicated to V.V. Minin on the occasion of his 80th birthday

Copper(II) Trimethylacetate Complex with Caffeine: Synthesis, Structure, and Biological Activity

D. S. Yambulatov[a, *], S. A. Nikolaevskii[a], I. A. Lutsenko[a], M. A. Kiskin[a], M. A. Shmelev[a], O. B. Bekker[b], N. N. Efimov[b], E. A. Ugolkova[a], V. V. Minin[a], A. A. Sidorov[a], and I. L. Eremenko[a, c]

[a] *Kurnakov Institute of General and Inorganic Chemistry, Russian Academy of Sciences, Moscow, 119991 Russia*

[b] *Vavilov Institute of General Genetics, Russian Academy of Sciences, Moscow, 119991 Russia*

[c] *Nesmeyanov Institute of Organoelement Compounds, Russian Academy of Sciences, Moscow, Russia*

**e-mail: yambulatov@yandex.ru*

Received June 9, 2020; revised June 15, 2020; accepted June 17, 2020

Abstract—The reaction of copper(II) trimethylacetate, $[Cu(Piv)_2]_n$ (Piv = $C(Me)_3COO^-$), with caffeine (L) (Cu : L = 1 : 1) in anhydrous acetonitrile yielded the binuclear complex $[Cu_2(Piv)_4(L)_2] \cdot 2CH_3CN$ (**I**). The structure of the complex in the crystal was established by X-ray diffraction (CIF file CCDC no. 2006753), and the electronic structure was studied by ESR. The effect of caffeine coordination to the biogenic complexing agent was established: the in vitro biological activity of the obtained complex towards the non-pathogenic strain *Mycolicibacterium smegmatis* was eight times higher than that of free caffeine.

Keywords: caffeine, ESR, copper(II) complex, carboxylate, biological activity

DOI: 10.1134/S1070328420110093

INTRODUCTION

Copper is one of the most important minor nutrients in the human body; it is involved in oxygen transfer and storage processes and in the regulation of oxidation processes in proteins [1]. Copper ions form complexes with various ligands and interact with biomolecules, mainly proteins and nucleic acids [2]. Copper complexes are active against various cancer cells [3–5] and suppress multiplication of some bacteria: salmonellas [6] and *E. coli* [7, 8].

A trend of modern bioinorganic chemistry is using simple biologically active molecules such as purine bases (theobromine, theophyllin, and caffeine) as ligands [9]. Caffeine is known to be a medicinal agent [10] and to perform a significant role in human life [11]. The platinum compound $[P(C_6H_5)_3(CH_3)][PtCl_3(L)]$, exhibiting antitumor activity in vivo, can be regarded as one of the first biologically active complexes involving caffeine, that is, 1,3,7-trimethyl-1H-purine-2,6(3H,7H)-dione (L) [12]. Recently it was shown that free caffeine has a slight cytotoxicity, while gold(I) complexes with L show high and selective cytotoxicities against various types of cancer cells [13]. Moreover, in vitro cyto- and genotoxicities were found for simple zinc complexes $[ZnL(H_2O)(Hal)_2]$ (Hal = Cl, Br, I) and for cadmium complexes $\{[Cd(H_2O)_2I_2] \cdot L \cdot 2H_2O\}_n$ [14, 15].

Carboxylate anions are convenient ligands, which, together with donor molecules, can control the formation of particular molecular or even polymeric metal cores of complexes [16–20]. In addition, depending on the nature of substituents in the carboxylate anions and on their electric and geometrical characteristics, one can expect biophysical properties for these molecules [1]. An example of such carboxylate ligands is α-furancarboxylic acid (2-furoic acid, HFur), whose nitro derivatives are incorporated in antimicrobial pharmaceutical products (furazolidone, furadonin, quinifuryl). It is known that some transition metal complexes with 2-furoic acid anions are also biologically active. Recent studies demonstrated that the heterometallic carboxylate complex $[Fe_2CoO(Fur)_6(THF)(H_2O)_2]$, containing anions of this acid, shows activity against the virulent strain *Mycobacterium tuberculosis* H37Rv and a weak cytotoxicity [21]. In addition, mono- and binuclear zinc, copper(II), and cobalt(II) complexes with α-furancarboxylate anions and various N-donor ligands were biologically active in vitro against the non-pathogenic strain *M. smegmatis*, with the activity being up to 50 times higher than that of the free acid [22, 23].

The purpose of this study was to prepare copper(II) trimethylacetate complex containing no biogenic α-furancarboxylate anions, but containing caffeine, a biologically active N-donor ligand, to determine the crystal and electronic structures of this compound, to study the biological properties towards to *M. smegmatis*, and to compare the results with those for free caffeine. Note that in the known studies devoted to caffeine complexes, the authors paid attention to the structure [24–29], magnetic properties [30–32], and their correlation [33, 34], but the biological activity of these compounds was reported only in a few publications [9, 35, 36].

EXPERIMENTAL

The target product was synthesized and isolated under anhydrous conditions using the standard Schlenck technique. Acetonitrile (reagent grade, Khimmed) was dried with phosphorus(V) oxide, stored with activated molecular sieves (4 Å), and withdrawn by condensation just before the synthesis. Anhydrous copper(II) trimethylacetate, $[Cu(Piv)_2]_n$, was prepared similarly to $[Co(Piv)_2]_n$ [37] from copper(II) acetate monohydrate (reagent grade, Ruskhim) in a HPiv melt; the product was kept in a dynamic vacuum at 120°C for 10 h. Caffeine (99%, Alfa Aesar) was used as received.

Attenuated total reflectance (ATR) IR spectrum of the product was recorded in the 400–4000 cm^{-1} range on a Perkin Elmer Spectrum 65 spectrophotometer equipped with a Quest ATR Accessory (Specac). Elemental analysis was carried out on an automated EuroEA-3000 C,H,N,S analyzer (EuroVektor).

The ESR spectra were measured on a Bruker ELEXSYS E-680X instrument in the X-range at T = 300 K. The parameters of all ESR spectra were found using the best fit method between experimental and theoretical spectra by minimizing the error functional:

$$F = \frac{\sum_i (Y_i^T - Y_i^E)^2}{N}, \quad (1)$$

where Y_i^E is the set of experimental ESR signal intensities with a constant step in the magnetic field H, Y_i^T are the theoretical values at the same field strengths H, and N is the number of points. The ESR spectra were simulated using the eigenfield method [38]. The theoretical spectrum of the solution was simulated as reported previously [39]. According to the relaxation theory [40], the line width was specified by the expression

$$\sigma = \alpha + \beta m_I + \gamma m_I^2, \quad (2)$$

where m_I is the projection of the nuclear spin on the magnetic field direction, while, α, β and γ are line width parameters. The sum of the Lorentz and Gauss functions was used as the line shape function [41]. During minimization, *g*-factors, HFS constants, and line widths and shapes were varied.

The biological activity was determined using the *M. smegmatis* mc^2 155 test system with paper discs. The test included determination of the zone of growth inhibition for the bacterial lawn inoculated on an agarized medium around paper discs containing the test compound in various concentrations. The bacteria washed from Petri dishes with the M-290 tryptone soya agar medium (Himedia) were grown overnight in the Lemco-TW liquid medium (Lab Lemco' Powder 5 g/L (Oxoid), Peptone special 5 g/L (Oxoid), NaCl 5 g/L, Tween-80) at 37°C up to the mid logarithmic growth phase at the optical density OD600 = 1.5, and mixed with the molten M-290 agarized medium in 1 : 9 : 10 ratio (culture : Lemco-TW : M-290). The culture was incubated for 24 h at 37°C. The minimum concentration giving rise to a growth inhibition zone was taken as the minimum inhibitory concentration (MIC).

Synthesis of $[Cu_2(Piv)_4L_2] \cdot 2MeCN$ (I). Weighed portions of $[Cu(Piv)_2]_n$ (0.265 g, 1.0 mmol) and caffeine (0.194 g, 1.0 mmol) were placed into a glass ampoule and degassed in a dynamic vacuum for 20 min, acetonitrile (15 mL) was condensed into the ampoule, and the ampoule was sealed and heated on an oil bath at 130°C until the reactants completely dissolved (1 h). The green-colored reaction mixture was cooled (10°C/h) to 60°C. During cooling, crystals were formed. Maintenance at this temperature (3 h) and further cooling to room temperature resulted in the formation of green crystals shaped as hexagonal prisms. The yield was 0.460 g (92%).

For $C_{40}H_{62}N_{10}O_{12}Cu_2$			
Anal. calcd., %	C, 47.94	H, 6.24	N, 13.98
Found, %	C, 47.89	H, 6.11	N, 13.86

IR (ATR; ν, cm^{-1}): 3132 w, 2984 w, 2959 m, 2932 w, 2903 w, 2868 w, 2245 w, 1708 m, 1665 vs, 1607 vs, 1568 s, 1505 m, 1482 s, 1455 m, 1440 m, 1417 vs, 1378 m, 1363 m, 1326 w, 1284 w, 1226 s, 1184 m, 1084 w, 1032 m, 980 w, 930 w, 897 w, 856 w, 799 w, 789 m, 762 m, 747 s, 612 s, 487 m.

Single crystal X-ray diffraction study of compound **I** was performed on a Bruker Apex II diffractometer equipped with a CCD array detector (MoK_α, λ = 0.71073 Å, graphite monochromator) [42]; semiempirical absorption corrections were applied by the SADABS software program [43]. The structure was solved by the direct methods and refined by full-matrix least squares method in the anisotropic approximation for all non-hydrogen atoms. The hydrogen atoms attached to carbons of the organic ligands were generated geometrically and refined in the riding model. The calculations were carried out using the SHELX [44] and OLEX2 [45] software.

Crystallographic parameters and structure refinement details for **I** at $T = 100(2)$ K: $C_{40}H_{62}N_{10}O_{12}Cu_2$, M = 1002.07 g/mol, space group $P2_1/n$, 0.1 × 0.2 ×0.2 mm rhombic green crystals, a = 12.2676(5), b = 15.6847(6), c = 12.6737(5) Å, β = 101.051(2)°, V = 2393.37(16) Å^3, Z = 2, ρ(calcd.) = 1.390 g cm^{-3}, μ = 0.956 mm^{-1}, 2.570° ≤ θ ≤ 30.503°, sphere segment −15 ≤ h ≤ 15, −19 ≤ k ≤ 19, −15 ≤ l ≤ 15, 21979 measured reflections, 4675 unique reflections, 3958 reflections with $I > 2\sigma(I)$, Rint = 0.0496, GOOF = 1.047, R1 ($I > 2\sigma(I)$) = 0.0467, wR2 ($I > 2\sigma(I)$) = 0.0906, R1 (all data) = 0.0581, wR2 (all data) = 0.947, Δρmin/Δρmax, e Å−3 = −0.483/0.581. The geometry of the metal polyhedra was determined using the SHAPE 2.1 software [46, 47].

The structural data were deposited with the Cambridge Crystallographic Data Centre (CCDC no. 2006753; deposit@ccdc.cam.ac.uk or http://www.ccdc.cam.ac.uk/data_request/cif).

RESULTS AND DISCUSSION

The reaction of equimolar amounts of anhydrous copper(II) pivalate and caffeine gave the crystals of the dimeric complex $[Cu_2(Piv)_4L_2] \cdot 2MeCN$ (**I**) in a practical yield of 92% (Scheme 1). In this reaction, $[Cu(Piv)_2]_n$ is dissolved in MeCN to give $[Cu_2(Piv)_4(MeCN)_2]$ [48], in which labile solvent molecules have been replaced by monodentate caffeine molecules.

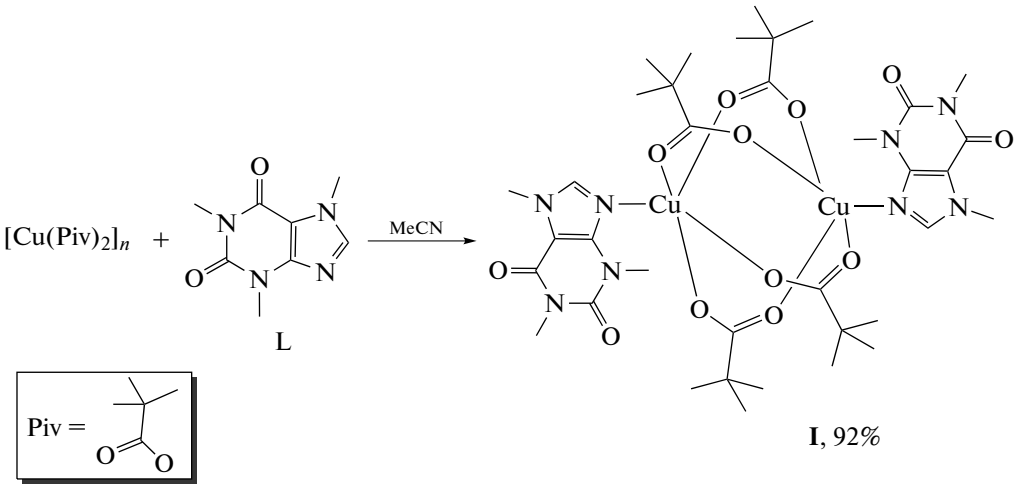

Scheme 1.

Complex **I** crystallizes in the monoclinic space group $P2_1/n$ with two acetonitrile solvent molecules (Fig. 1). The molecule of the complex is symmetric, with the inversion center being located between the Cu(1) and Cu(1A) atoms. The metal atoms are linked by four bridging carboxylate groups (Cu–O, 1.955(2)–1.970(2) Å; Cu...Cu, 2.6219(5) Å). The apical ligand (caffeine molecule) is coordinated in the monodentate fashion via the imidazole N atom (Cu–N 2.234(2) Å). The ligand retains a planar structure, the dihedral angle between the pyrimidine and imidazole rings is 1.3°; the most pronounced deviation of atoms from the root-mean-square plane is observed for N(1) (0.025(1) Å) and O(5) (0.057(1) Å). The coordination environment of copper ($CuNO_4$) corresponds to a square pyramid (τ(Cu) = 0 [49]), in which the square geometry of the base is virtually retained, as evidenced by similar values of the OCuO angles (O(1)Cu(1)O(3), 90.6(1)°; O(2)Cu(1)O(3), 88.60(9)°; O(2)Cu(1)O(3), 88.94(9)°; O(1)Cu(1)-O(4) 89.53(10)°).

In the molecule of complex **I**, the N(1)–Cu(1)...Cu(1)–N(1) moiety deviates from linearity (the N(1)Cu(1)Cu(1) angle is 171.67(6)°). The Cu(1) atom deviates from the plane of four oxygen atoms (O(1),O(2),O(3),O(4)) by 0.198 Å towards the N(1) atom of caffeine. The bridging carboxylate groups are unsymmetrical, since the pair of O atoms is located near the pyrimidine moiety. As a result, two OCuN angles are greater than 90° (O(1)Cu(1)N(1) 102.20(8)°, O(4)Cu(1)N(1) 99.31(8)°). The OCuN angles at the O atoms that are not affected by the bulky substituent L do not differ much from the right angle: (O(2)Cu(1)N(1) 89.35(8)°, O(3)Cu(1)N(1) 92.07(8)°).

The relative positions of the caffeine aromatic systems of neighboring molecular moieties in the crystal packing attest to intermolecular π–π-interaction, giving rise to supramoleculear chains in complex **I** (the distance between the centroids of pyrimidine moieties and the angle between the planes are 3.3808(15) Å and 0.00(12)°, respectively) (Fig. 2).

The formation of binuclear tetrabridged structures is typical of copper(II) complexes with monocarboxylate anions and caffeine, in which the latter acts as a monodentate N-donor [24–26, 28, 29, 31, 32, 34] or

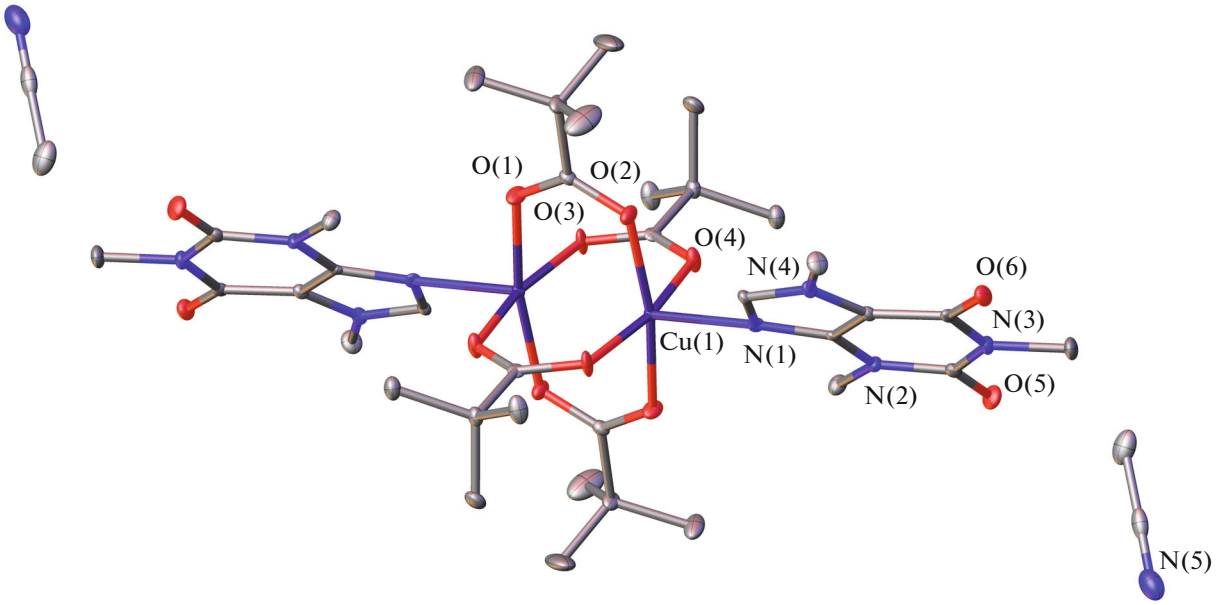

Fig. 1. Molecular structure of complex **I**; thermal ellipsoids are drawn at the 35% probability level. The hydrogen atoms are omitted.

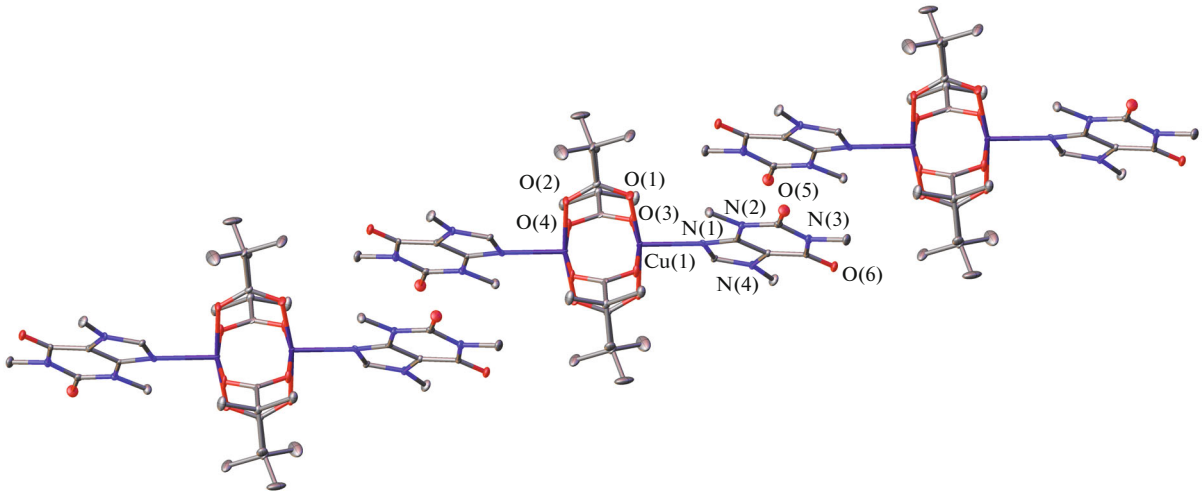

Fig. 2. Fragment of the packing of complex **I**; thermal ellipsoids are drawn at the 35% probability level. The hydrogen atoms and solvate molecules are omitted.

O-donor [50] ligand. Currently, there is only one known complex in which caffeine functions as a bridging N,O-donor ligand, binding the $\{Cu_2(\mu\text{-}O_2CR)_4L\}$ moieties into 1D polymer chain [33].

The Cu–O and Cu–N bond lengths and geometry distortion for complex **I** are comparable with the values for known complexes $[Cu_2(\mu\text{-}Piv)_4L'_2]$, where L' is pyridine [51], 2-aminopyridine [52], 2,3-cyclododecenopyridine [53], and quinoline [54] and for binuclear copper compounds with monocarboxylate anions and caffeine molecules $[Cu_2(\mu\text{-}O_2CR)_4L_2]$, where O_2CR are monochloroacetate [24], benzoate [34], 2-bromopropionate [29], 2-iodobenzoate [26], 6-methoxy-α-methyl-2-naphthaleneacetate [25], and 2-formylbenzoate [31] anions. A more pronounced geometric distortion of the metal core than in complex **I** was found for compound $[Cu_2(O_2CCCl_3)_4L_2]$ [33], in which the angle CuCuN decreases to 156.89°, the Cu–Cu distance markedly increases to become 3.062 Å, while the Cu–N decreases to 2.046 Å.

The ESR spectrum of a finely dispersed powder of complex **I** (Fig. 3a) is typical of an axially symmetrical complex with the total spin $S = 1$ and is described by spin Hamiltonian (SH) with the fine structure:

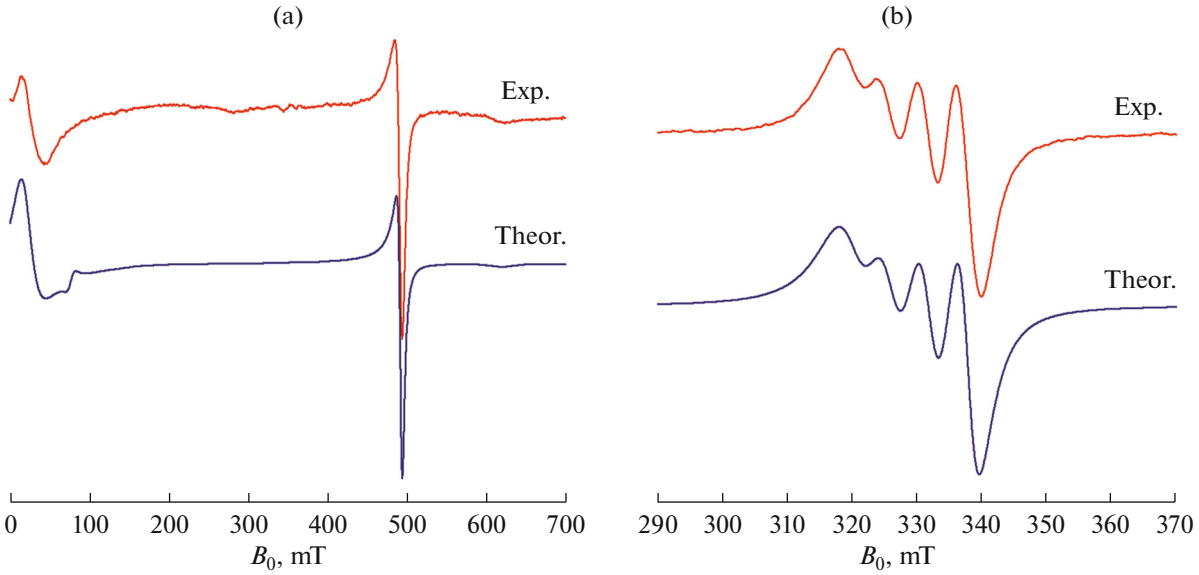

Fig. 3. Experimental and theoretical ESR spectra of (a) fine powder and (b) a dichloromethane–pyridine (20 : 1) solution of complex **I** at 300 K. Parameters of the simulated spectra are given in the text.

$$H = \beta\left(g_x S_x H_x + g_y S_y H_y + g_z S_z H_z\right) + D\left(S_z^2 - \frac{S(S+1)}{3}\right), \quad (3)$$

where $S = 1$; S_x, S_y, S_z are the projections of the total spin on the *x, y,* and *z* axes, respectively; D is a component of the fine coupling tensor; g_x, g_y, g_z are *g*-tensor components; H is the magnetic field strength. The SH parameters (3) of the best fit between the experimental and simulated spectrum of a powder of compound **I** were as follows: $|D| = 0.3479$ cm^{-1}, $g_z = g_\parallel = 2.340$, $g_x = g_y = g_\perp = 2.055$ (Fig. 3a).

Upon dissolution of complex **I** in dichloromethane, no ESR spectrum is observed. The addition of pyridine gives rise to an isotropic ESR spectrum with a hyperfine structure (HFS) consisting of four lines (Fig. 3b). This spectrum is characteristic of mononuclear copper(II) complexes. The ESR spectrum of the mononuclear complex formed upon dissolution of **I** in a dichloromethane–pyridine mixture (20 : 1) at room temperature is described by isotropic SH with the total spin $S = 1/2$ and Zeeman and hyperfine coupling:

$$H = g\beta HS + aSI, \quad (4)$$

where g is a *g*-tensor component, β is the Bohr magneton, a is a component of the HFS tensor, $S = 1/2$, $I = 3/2$. The best fit of the simulated spectrum to the experimental one for mononuclear fragments gave the following parameters for SH (4): $g = 2.141$, $a = 5.81 \times 10^{-3}$ cm^{-1} (Fig. 3b).

The antibacterial activity of compound **I** was assessed with respect to *M. smegmatis*. This strain is used for screening antituberculosis drugs, as it is nonpathogenic (used in laboratory without additional protection levels), grows faster than other types of mycobacteria, and is sensitive to clinically used antituberculosis drugs [55, 56]. It is known that the chemotherapeutic drug resistance of mycobacteria is caused by low permeability and unusual structure of the mycobacterial cell wall. The *M. smegmatis* test system has a higher antibiotic and antituberculosis drug resistance than *M. tuberculosis*; therefore, the compound concentration of <100 nmol/disc served as the selection criterion, unlike that in the case of *M. tuberculosis* [57]. The test method included quantification of the diameter of the zone of growth inhibition for the *M. smegmatis* culture grown as a lawn on an agarized medium around paper discs impregnated with test compounds. The test complex was deposited on the discs in various concentrations. The halo diameter (growth inhibition zone) was found to increase with increasing amount of the compound deposited on the disc. The MIC concentration of the compound was that producing the minimum visible growth inhibition: the lower the MIC, the more active the compound. The results of antibacterial activity assays in the *M. smegmatis* mc^2 155 test system and its variation with time are summarized in Table 1. As follows from the data of Table 1, the MIC for free caffeine is 2000 nmol/disc, indicating that the activity against *M. smegmatis* is almost absent (the growth inhibition zone is overgrown almost immediately). The caffeine coordination to Cu^{2+} increases the biological activity by a factor of eight and provides a more persistent bacteriostatic effect. For comparison, Table 1 presents the biological activity data for some copper(II) furoate complexes with various N-donor ligands [22, 23]. Presumably, a copper compound with two different bio-

Table 1. Antibacterial activity against *Mycolicibacterium smegmatis* mc^2 155

Compound*	MIC, nmol/disc	MIC, μg/disc	Inhibition zone, mm	
			24 h	120 h
I	250	250	6.5**	0
[Cu(α-Fur)$_2$(Phen)] [22]	5	2	7.0***	7.0***
[Cu(α-Fur)$_2$(Bipy)(H$_2$O)] [23]	100	46	7.0***	7.0***
[Cu$_2$(α-Fur)$_4$(Py)$_2$] [22]	200	146	7.0**	7.0**
[Cu(α-Fur)$_2$(Py)$_2$(H$_2$O)] [22]	400	153	7.0**	7.0**
Isoniazid	700	100	9.0	6.5***
Rifampicin	12	10	7.0	7.0***
Caffeine	2000	388	0****	0****

* Phen = 1,10-phenanthroline; Bipy = 2,2'-bipyridine; Py = pyridine. ** The inhibition zone of the bacterial growth that appeared after several hours of growth started to be covered over the whole surface. *** The diameter of the inhibition zone of culture growth does not change over the indicated time interval. **** The growth inhibition zone is absent.

logically active ligands (α-furancarboxylate anion, caffeine) may surpass the compounds evaluated here.

Thus, a new binuclear copper(II) trimethylacetate complex with caffeine was synthesized and its molecular and crystal structure was determined. According to ESR results, the complex has the total spin $S = 1$, which in turn confirms its binuclear structure and the presence of magnetic interactions between copper ions in the molecule. It was shown that compound **I**, unlike free caffeine, shows biological activity in vitro against *M. smegmatis* bacteria.

ACKNOWLEDGMENTS

The X-ray diffraction analysis, elemental analysis, IR and ESR spectroscopy measurements were performed using shared experimental facilities supported by IGIC RAS state assignment.

FUNDING

This work was supported by the Russian Science Foundation (Project 20-13-00061).

CONFLICT OF INTEREST

The authors declare that they have no conflicts of interest.

REFERENCES

1. Jones, C.J. and Thornback, J.R., *Medicinal Applications of Coordination Chemistry*, The Royal Society of Chemistry, 2007.
2. Iakovidis, I., Delimaris, I., and Piperakis, S.M., *Mol. Biol. Int.*, 2011, vol. 2011, ID 594529.
3. Trávníček, Z., Maloň, M., Šindelář, Z., et al., *J. Inorg. Biochem.*, 2001, vol. 84, p. 23.
4. Daniel, K.G., Gupta, P., Harbach, R.H., et al., *Biochem. Pharmacol.*, 2004, vol. 67, p. 1139.
5. Marengo, A., Forciniti, S., Dando, I., et al., *Biochim. Biophys. Acta Gen. Subjects*, 2019, vol. 1863, p. 61.
6. Mekahlia, S. and Bouzid, B., *Phys. Procedia*, 2009, vol. 2, p. 1045.
7. Sousa, I., Claro, V., Pereira, J.L., et al., *J. Inorg. Biochem.*, 2012, vol. 110, p. 64.
8. Efthimiadou, E.K., Thomadaki, H., Sanakis, Y., et al., *J. Inorg. Biochem.*, 2007, vol. 101, p. 64.
9. Melník, M., Sprusansky, O., and Musil, P., *Adv. Biol. Chem.*, 2014, vol. 4, p. 274.
10. *European Pharmacopoeia,6.2*, Strasbourg: Council of Europe, 2007.
11. Preedy, V.R., *Caffeine Chemistry, Analysis, Function and Effects*, The Royal Society of Chemistry, 2012.
12. Cramer, R.E., Ho, D.M., Van Doorne, W., et al., *Inorg. Chem.*, 1981, vol. 20, p. 2457.
13. Trommenschlager, A., Chotard, F., Bertrand, B., et al., *ChemMedChem*, 2018, vol. 13, p. 2408.
14. Rukk, N.S., Kuzmina, L.G., Shamsiev, R.S., et al., *Inorg. Chim. Acta*, 2019, vol. 487, p. 184.
15. Rukk, N.S., Kuz'mina, L.G., Davydova, G.A., et al., *Mendeleev Commun.*, 2019, vol. 29, p. 640.
16. Nikolaevskii, S.A., Evstifeev, I.S., Kiskin, M.A., et al., *Polyhedron*, 2018, vol. 152, p. 61.
17. Kiskin, M.A. and Eremenko, I.L., *Russ. Chem. Rev.*, 2006, vol. 75, p. 559.
18. Sidorov, A.A., Kiskin, M.A., Aleksandrov, G.G., et al., *Russ. J. Coord. Chem.*, 2016, vol. 42, p. 621. https://doi.org/10.1134/S1070328416100031
19. Nikolaevskii, S.A., Yambulatov, D.S., Starikova, A.A., et al., *Russ. J. Coord. Chem.*, 2020, vol. 46, p. 260. https://doi.org/10.1134/S1070328420040053
20. Zorina-Tikhonova, E.N., Yambulatov, D.S., Kiskin, M.A., et al., *Russ. J. Coord. Chem.*, 2020, vol. 46, p. 75. https://doi.org/10.1134/S1070328420020104
21. Melnic, S., Prodius, D., Stoeckli-Evans, H., et al., *Eur. J. Med. Chem.*, 2010, vol. 45, p. 1465.
22. Lutsenko, I.A., Baravikov, D.E., and Kiskin, M.A., *Russ. J. Coord. Chem.*, 2020, vol. 46, no. 6, p. 411. https://doi.org/10.1134/S1070328420060056

23. Lutsenko, I.A., Yambulatov, D.S., Kiskin, M.A., et al., *Russ. J. Coord. Chem.*, 2020, vol. 46 (in the press).
24. Koreň, B., Valach, F., Sivý, P., and Melník, M., *Acta Crystallogr., Sect. C: Cryst. Struct. Commun.*, 1985, vol. 41, p. 1160.
25. Koman, M., Melník, M., Moncol' J., and Glowiak, T., *Inorg. Chem. Commun.*, 2000, vol. 3, p. 489.
26. Valach, F., Tokarčík, M., Maris, T., et al., *J. Organomet. Chem.*, 2001, vol. 622, p. 166.
27. Valach, F., Melník, M., Bernardinelli, G., and Fromm, K.M., *J. Chem. Crystallogr.*, 2006, vol. 36, p. 571.
28. Ma, Z. and Moulton, B., *Mol. Pharm.*, 2007, vol. 4, p. 373.
29. Valach, F., Tokarčík, M., and Melník, M., *J. Coord. Chem.*, 2009, vol. 62, p. 225.
30. Horie, H., Husebye, S., Kato, M., et al., *Acta Chem. Scand. A*, 1986, vol. 40, p. 579.
31. Harada, A., Tsuchimoto, M., Ohba, S., et al., *Acta Crystallogr., Sect. B: Struct. Sci.,* 1997, vol. 53, p. 654.
32. Melník, M., Koman, M., and Glowiak, T., *Polyhedron*, 1998, vol. 17, p. 1767.
33. Uekusa, H., Ohba, S., Tokii, T., et al., *Acta Crystallogr., Sect. B: Struct. Sci.*, 1992, vol. 48, p. 650.
34. Kawata, T., Uekusa, H., Ohba, S., et al., *Acta Crystallogr., Sect. B: Struct. Sci.*, 1992, vol. 48, p. 253.
35. Dudová, B., Hudecová, D., Pokorný, R., et al., *Folia Microbiol.* (Praha), 2001, vol. 46, p. 379.
36. Dudová, B., Hudecová, D., Pokorný, R., et al., *Folia Microbiol.* (Praha), 2002, vol. 47, p. 225.
37. Fomina, I.G., Aleksandrov, G.G., Dobrokhotova, Z.V., et al., *Russ. Chem. Bull.*, 2006, vol. 55, p. 1909.
38. Belford, G.G., Belford, R.L., and Burkhalter, J.F., *J. Magn. Reson.*, 1973, vol. 11, p. 251.
39. Rakitin, Yu.V., Larin, G.M., and Minin, V.V., *Interpretatsiya spektrov EPR koordinatsionnykh soedinenii* (Interpretation of the ESR Spektra of Coordination Compounds), Moscow: Nauka, 1993.
40. Wilson, R. and Kivelson, D., *J. Chem. Phys.*, 1966, vol. 44, p. 154.
41. Lebedev, Ya.S. and Muromtsev, V.I., *EPR i relaksatsiya stabilizirovannykh radikalov* (ESR and Relaxation of Stabilized Radicals), Moscow: Khimiya, 1972.
42. Krause, L., Herbst-Irmer, R., Sheldrick, G.M., and Stalke, D., *J. Appl. Crystallogr.*, 2015, vol. 48, p. 3.
43. Sheldrick, G.M., SADABS, Madison: Bruker AXS Inc., 1997.
44. Sheldrick, G.M., *Acta Crystallogr., Sect. A*: *Found. Adv.*, 2015, vol. 71, p. 3.
45. Dolomanov, O.V., Bourhis, L.J., Gildea, R.J., et al., *J. Appl. Crystallogr.*, 2009, vol. 42, p. 339.
46. Alvarez, S. and Llunell, M., *Dalton Trans.*, 2000, p. 3288.
47. Casanova, D., Llunell, M., Alemany, P., and Alvarez, S., *Chem.-Eur. J.*, 2005, vol. 11, p. 1479.
48. Uvarova, M.A., Sinelshchikova, A.A., Golubnichaya, M.A., et al., *Cryst. Growth Des.*, 2014, vol. 14, p. 5976.
49. Addison, A.W., Rao, T.N., Reedijk, J., et al., *Dalton Trans.*, 1984, p. 1349.
50. Stachova, P., Moncol, J., Valigura, D., and Lis, T., *Acta Crystallogr., Sect. C: Cryst. Struct. Commun.*, 2006, vol. 62, p. m375.
51. Blewett, G., Esterhuysen, C., Bredenkamp, M.W., and Koch, K.R., *Acta Crystallogr., Sect. E: Struct. Rep. Online*, 2006, vol. 62, p. m420.
52. Fomina, I.G., Dobrokhotova, Z.V., Aleksandrov, G.G., et al., *Russ. Chem. Bull.*, 2010, vol. 59, p. 1175.
53. Gogoleva, N.V., Aleksandrov, G.G., Pavlov, A.A., et al., *Russ. J. Coord. Chem.*, 2018, vol. 44, p. 91. https://doi.org/10.1134/S1070328418020057
54. Fomina, I.G., Dobrokhotova, Z.V., Aleksandrov, G.G., et al., *Russ. Chem. Bull.*, 2007, vol. 56, p. 1722.
55. Yagi, A., Uchida, R., Hamamoto, H., et al., *J. Antibiot.* (Tokyo), 2017, vol. 70, p. 685.
56. Ramón-García, S., Ng, C., Anderson, H., et al., *Antimicrob. Agents Chemother.*, 2011, vol. 55, p. 3861.
57. Bekker, O.B., Sokolov, D.N., Luzina, O.A., et al., *Med. Chem. Res.*, 2015, vol. 24, p. 2926.

Translated by Z. Svitanko